

# Cluster Catch Digraphs with the Nearest Neighbor Distance

Rui Shi\*, Nedret Billor† and Elvan Ceyhan‡

## Abstract

We introduce a new method for clustering based on Cluster Catch Digraphs (CCDs). The new method addresses the limitations of RK-CCDs by employing a new variant of spatial randomness test that employs the nearest neighbor distance (NND) instead of the Ripley’s  $K$  function used by RK-CCDs. We conduct a comprehensive Monte Carlo analysis to assess the performance of our method, considering factors such as dimensionality, data set size, number of clusters, cluster volumes, and inter-cluster distance. Our method is particularly effective for high-dimensional data sets, comparable to or outperforming KS-CCDs and RK-CCDs that rely on a KS-type statistic or the Ripley’s  $K$  function. We also evaluate our methods using real and complex data sets, comparing them to well-known clustering methods. Again, our methods exhibit competitive performance, producing high-quality clusters with desirable properties.

**Keywords:** Graph-based clustering, Cluster catch digraphs, High-dimensional data, The nearest neighbor distance, Spatial randomness test.

## 1 Introduction

Clustering is a fundamental statistical and data analysis method, partitioning observations into groups based on similarity or proximity. Clustering is considered an unsupervised version of classification, and the primary goal is to understand the inherent structure of data, which plays a crucial role in machine learning and pattern recognition. Clustering faces challenges like determining the optimal number of clusters and handling high-dimensional data. Driver and Kroeber first introduced cluster analysis in 1932 [15], applying it to

---

\*The Department of Mathematics and Statistics, Auburn University, rzs0112@auburn.edu

†The Department of Mathematics and Statistics, Auburn University, billone@auburn.edu

‡The Department of Mathematics and Statistics, Auburn University, ezc0066@auburn.edu

anthropology. Early clustering methods focused on  $k$ -means and hierarchical methods, which are the fundamental of cluster analysis [54, 35]. Since then, clustering methods have evolved substantially and are widely used across different disciplines. Common examples include partitioning customers into distinct groups for better market strategy [60], grouping genes that have a similar physiological expression in Biology [18], enhancing image processing by dividing and re-grouping [12], and predicting human behavior based on their communities and social ties [25]. Despite significant advancements, clustering remains challenging, such as determining the optimal number of clusters [39], scalability to large data sets [67], robustness to outliers and noise [51], and handling high-dimensional data [6].

We propose clustering methods based on *Cluster Catch Digraphs* (CCDs). CCDs were first introduced by DeVinney [14] and Marchette [38], developed from a similar classification digraph called *Class Cover Catch Digraphs* (CCCDs). Later, Manukyan and Ceyhan [36] modified and improved this approach further, developing two variants using a Kolmogorov-Smirnov (KS) based statistic and Ripley’s  $K$  function, calling them KS-CCDs and RK-CCDs, respectively, RK-CCDs and KS-CCDs work similarly in clustering, and RK-CCDs are almost parameter-free, making them especially appealing. However, our experimental analysis shows that RK-CCDs may not be suitable for moderate to high dimensionality due to the limitation of the *Spatial Randomness Monte Carlo Test* (SR-MCT) based on Ripley’s  $K$  function [53]. Thus, we introduce another CCD-based approach that uses *Nearest Neighbors Distance* (NND) instead of Ripley’s  $K$  function to test underlying point-process patterns, and the resulting methods are called UN-CCDs [53]. Like RK-CCDs, UN-CCDs are almost parameter-free. We introduce the U-MCCD and SU-MCCD methods for outlier detection[53], which are based on RK-CCDs and UN-CCDs, respectively. We have shown that the SU-MCCD method performs comparably to the U-MCCD method when the number of dimensions  $d \leq 5$ , and outperforms it substantially when  $d \geq 10$ . Then, we propose two “flexible” variations of U-MCCDs and SU-MCCDs, called UN-MCCDs and SUN-MCCDs, respectively, aiming at outlier detection on the data sets with arbitrary-shaped clusters and varying intensities.

## 2 Literature and Background Review

So far, cluster-based methods have been classified into several subgroups, known as partitioning, hierarchical, density-based, grid-based, fuzzy-based, model-based, and distribution-based clustering methods.

### 2.1 Partitioning-Based Clustering Methods

Partitioning or distance-based clustering methods follow an iterative process [57], dividing a data set into single-level partitions, which differ from the hierarchical structure obtained by other clustering techniques [62]. These methods typically start with a pre-defined number of clusters, often represented by their centers, obtained through a simple method like random selection. The partitions are then iteratively refined until a specific criterion, typically the sum of squares of within-cluster (or inter-cluster) distances, is minimized (maximized). Partition-based clustering methods divide a data set into meaningful partitions for subsequent analysis [62]. While efficient and simple, they are sensitive to outliers and require the number of clusters as an input parameter [62]. Commonly known partition-based clustering methods include *K-Means* [24], *MacQueen* [35], *Partitioning Around Medoids* (PAM) [33], *Clustering LARge Applications* (CLARA) [33], and *Clustering Large Applications based on RANdomized Search* (CLARANS) [41].

### 2.2 Hierarchical Clustering Methods

The performance of partitioning-based clustering methods depends on the chosen number of clusters  $k$ . Determining the optimal value for  $k$  can be difficult when there is limited knowledge about the data set. Fortunately, *hierarchical clustering methods* offer a solution to this issue. Typically, these methods construct a hierarchical tree-like structure known as *dendrogram*, which allows for partitioning the whole data set at varying levels of granularity. Hierarchical clustering methods can be classified into two categories: *agglomerative* and *divisive clustering* [65]. Agglomerative clustering begins by treating each point as a cluster, merging the two closest clusters iteratively until a pre-defined stopping criterion is satisfied. Divisive clustering operates oppositely, treating the entire data set as a single cluster and partitioning iteratively.

Hierarchical clustering is versatile and can be applied to various types of data. The dendrogram provides a visual summary of the clustering process, increasing interpretabil-

ity. However, hierarchical clustering can be computationally expensive, especially for large data sets [45]. Commonly known hierarchical clustering methods includes *minimum variance method* [59], *Minimal Spanning Tree* [63], *Clustering Using Representatives (CURE)* [26], *CHAMELEON* [32], and *RObust Clustering using links (ROCK)* [27].

### 2.3 Density-Based Clustering Methods

The density-based clustering methods work similarly to the human eye, which identifies regions with high concentrations of data points as clusters. Like the hierarchical clustering methods, these methods do not require specifying the number of clusters. They can capture clusters of arbitrary shapes and sizes, exhibiting robustness to outliers. However, their performance depends on the input density parameters. Moreover, they may have difficulty identifying clusters under complex and high-dimensional data sets [20]. Recent density-based clustering methods include *Density-Based Spatial Clustering of Applications with Noise (DBSCAN)* [19], *Ordering Points To Identify the Clustering Structure (OPTICS)* [2], *Distribution Based Clustering of LArge Spatial Databases (DBCLASD)*, and *DENsity-based CLUstEring (DENCLUE)* [28].

### 2.4 Grid-Based Clustering Methods

Grid-based clustering methods operate by partitioning the data space into a finite number of cells, creating a grid structure. Clusters are then constructed based on these cells. Generally, the computational complexity depends on the granularity of the grid rather than the data size. Therefore, they can be efficient with large data sets and are suitable for arbitrarily shaped clusters thanks to their flexibility. However, the quality of clustering depends on the granularity. Moreover, they have difficulty capturing clusters with irregular boundaries [62]. Some well-known grid-based clustering methods include *STING* [58], *WaveCluster* [52], *DClust* [66], and *Clustering In QUEst (CLIQUE)* [1].

### 2.5 Model-Based Clustering Methods

Model-based (or distribution-based) clustering methods operate under the assumption that data is generated from a mixture of distributions, with each component representing a cluster. These methods aim to recover the models and parameters that best fit the observed data, constructing clusters based on the estimated models [45]. The major advantage of them is their flexibility to the cluster shapes and sizes, without requiring a

predetermined number of clusters. Moreover, they allow “soft” clustering, where a data point can belong to multiple clusters. However, model-based clustering methods can be computationally expensive, and the clustering quality highly depends on the parameters of the chosen models [62]. Some examples include *Gaussian Mixture Models* (GMMs) [46], *Latent Dirichlet Allocation* (LDA) [7], *Hidden Markov Models* (HMM) [44], *Expectation Maximization* (EM) [13], *COBWEB* [21], *pdfCluster* [4], and *SOM* [56].

## 2.6 Fuzzy Clustering

Fuzzy clustering methods, also known as “soft” clustering, allow data points to belong to two or more clusters simultaneously, each with an associated degree of membership [20]. This allows clusters to overlap and makes fuzzy clustering suitable for data sets with ambiguous and poorly separated cluster boundaries [33]. Additionally, these methods offer insights into the underlying data structure. However, the iterative optimization process on membership degrees can be computationally expensive [20].

We enumerate some fuzzy clustering methods: *Fuzzy C-means* (FCM) is another variant of *K-Means* and allows soft clustering [17]. However, it is sensitive to initial partition, not robust to outliers and noise, and can get trapped in a local optimum [50]. *Possibilistic-fuzzy C-means* (PFCM) combines *possibilistic C-means* (PCM) and FCM [42, 34]. Therefore, it is more robust to noise and outliers. *Kernelized Fuzzy C-means* (KFCM) is another variant of FCM [64], incorporating the kernel method to handle clusters with non-linear boundaries.

## 3 Preliminaries

### 3.1 Cluster Catch Digraphs

Our clustering methods are based on Cluster Catch Digraphs (CCDs), where vertices represent the points of a given data set  $\mathcal{X}$ , and arcs are determined by the spherical ball (covering ball) centered at each point. Class Cover Catch Digraphs (CCCDs) [43] are the prototypes of CCDs, originally designed for supervised classification. CCCDs aim to distinguish a target class from a non-target class by covering the target class points with a minimum number of open balls while excluding the non-target points [38]. A CCCD is constructed by creating covering balls around each point, forming arcs between points when one lies within the covering ball of another. Two variants, pure-CCCDs (P-CCCDs)

and random walk-CCCDs (RW-CCCDs), differ in how the radius of each covering ball is determined [36]. As in the CCD classification, to reduce the covering complexity in CCDs and avoid overfitting, we retain only a subset of covering balls that optimally covers all (or most) points in a data set. One way is finding a *minimum dominating set* (MDS) of the CCD. Although finding the MDS of a digraph is an NP-Hard problem [31], an efficient approximation of MDS can be found using the Greedy Algorithm, which operates in  $O(|V_0|^2)$  time [9, 29]. The Greedy Algorithm finds an approximate MDS by iteratively selecting the vertex with the highest outdegree, adding it to the dominating set, and removing its closed neighborhood (in the graph) from the uncovered vertices until all vertices are covered. Manukyan and Ceyhan proposed two variants of the Greedy Algorithm for CCDs [37]: the first variant prioritizes vertices closer to cluster centers, while the second maximizes a score function  $sc(v)$  at each step. We provide these methods in Algorithms 1 and 2, respectively, since they are non-standard in their greediness and also for future reference.

---

**Greedy Algorithm 1:** (A greedy algorithm finding an approximate MDS) This greedy algorithm is adapted for CCDs.  $V$  and  $A$  are the initial vertex and edge sets of the digraph  $D$ ;  $D^{sub}(S)$  is the induced sub-digraph of vertex set  $S$  from a digraph  $D$ ,  $\bar{N}(v)$  is the closed neighborhood of a vertex  $v$  (i.e., the points covered by the covering ball centered at  $v$ ).  $V_{temp}$  represents the uncovered vertices at current iteration.

---

**Input:** A digraph  $D = (V(D) = \mathcal{X}, A(D))$  where  $\mathcal{X} = \{x_1, x_2, \dots, x_n\}$

**Output:** A approximate minimum dominate set  $\hat{S}$

1 **Initialization:**  $V_{temp} \leftarrow V(D)$ ,  $V \leftarrow V(D)$ ,  $A \leftarrow A(D)$ ,  $\hat{S} \leftarrow \emptyset$

2 **while**  $V_{temp} \neq \emptyset$  **do**

3      $v_{temp} \leftarrow \arg \max_{v \in V \setminus \hat{S}} \{d_{out}^*(v)\};$              ( $d_{out}^*(v)$ : the outdegree of  $v$  in  $A$ )

4      $V_{temp} \leftarrow V_{temp} \setminus \bar{N}(v_{temp});$

5      $\hat{S} \leftarrow \hat{S} \cup \{v_{temp}\};$

6      $D \leftarrow D^{sub}(V_{temp});$

**end**

---

### 3.1.1 Cluster Catch Digraphs Using a KS-Type Statistic

CCDs, introduced by Devinney [14], are an adaptation of CCCDs [43] for unsupervised clustering. Given an unlabeled data set  $\mathcal{X} = \{x_1, x_2, \dots, x_n\} \subset \mathbb{R}^d$ , where points are drawn from a mixture distribution, the objective is to determine the number of clusters and the optimal data partitioning. Unlike CCCDs, CCDs determine the radius of each covering ball using a Kolmogorov-Smirnov (KS)-type statistic, which measures the deviation of the

---

**Greedy Algorithm 2:** A greedy algorithm finding an approximate MDS which is greedy in a score function  $sc(v)$  at each iteration.

---

**Input:** A digraph  $D = (V(D), A(D))$ . for a given data set  $\mathcal{X} = \{x_1, x_2, \dots, x_n\}$   
**Output:** A approximate minimum dominate set  $\hat{S}$ .  
**1 Initialization:**  $V_{temp} \leftarrow V(D)$ ,  $\hat{S} \leftarrow \emptyset$   
**2 while**  $V_{temp} \neq \emptyset$  **do**  
**3**      $v_{temp} \leftarrow \arg \max_{v \in V(D)} \{sc(v)\}$ ;                     $(sc(v):$ the score function for  $v)$   
**4**      $V_{temp} \leftarrow V_{temp} \setminus \bar{N}(v_{temp})$ ;  
**5**      $\hat{S} \leftarrow \hat{S} \cup \{v_{temp}\}$ ;  
**6**      $D \leftarrow D^{sub}(V_{temp})$ ;  
**end**

---

local density around each point  $x_i$  from a null model such as *Complete Spatial Randomness* (CSR) [38].

The KS-statistic for a point  $x_i$  is defined as:

$$T_{KS}(x_i, r) = F_{rw}(x_i, r) - F_0(x_i, r),$$

where  $F_{rw}(x_i, r)$  represents the number of points within the covering ball  $B(x_i, r)$  centered at  $x_i$  with radius  $r$ , and  $F_0(x_i, r)$  is the expected number of points under the null model, typically given by  $F_0(x_i, r) = \delta r^d$  for CSR, where  $\delta$  is a density parameter and  $d$  is the dimension of the space. The radius  $r_{x_i}$  is chosen to maximize  $T_{KS}(x_i, r)$ :

$$r_{x_i} = \arg \max_{r \geq 0} \{T_{KS}(x_i, r)\},$$

ensuring that the points covered by  $B(x_i, r_{x_i})$  form a significant local cluster.

Once the optimal radii  $r_{x_i}$  are determined for all points, a CCD for  $\mathcal{X}$  is constructed as a digraph  $D = (V(D), A(D))$ , where each vertex corresponds to a point in  $\mathcal{X}$ , and there is an arc from  $x_i$  to  $x_j$  if  $x_j \in B(x_i, r_{x_i})$ . The weakly connected components of  $D$  are taken as clusters.

To reduce the complexity of the covering, we apply the Greedy Algorithm 1 to find an approximate MDS, denoted  $\hat{S}$ , which selects a subset of covering balls to represent the clusters more efficiently [38]. The algorithm iteratively selects the vertex with the largest outdegree and removes its neighborhood until all points are covered.

To further reduce the complexity of the cluster cover, an *intersection graph*  $G_{MD} = (V_{MD}, E_{MD})$  is constructed, where  $V_{MD} = \hat{S}$ , and an edge exists between  $u, v \in \hat{S}$  if their covering balls cover common points, i.e.,  $N(u) \cap N(v) \neq \emptyset$ . The Greedy Algorithm 2 is

then applied to  $G_{MD}$  to prune the set  $\hat{S}$  further, yielding a reduced set  $\hat{S}(G_{MD})$  that represents the core clusters.

Finally, to refine the clustering further and remove noise or outlier clusters, the silhouette index  $sil(x_i)$  is used [23]. Clusters are added incrementally to the partition  $P = \{P_1, P_2, \dots, P_k\}$  until the average silhouette index  $sil(P)$  is maximized, ensuring only significant clusters are retained. The covering balls of the significant clusters are called dominating covering balls. Points not covered by any cluster are assigned based on the relative similarity measure  $\rho(x_i, B(x_j, r_{x_j}))$ :

$$\rho(x_i, B(x_j, r_{x_j})) = \frac{d(x_i, x_j)}{r_{x_j}},$$

where  $d(x_i, x_j)$  is the distance between  $x_i$  and the center  $x_j$  of the nearest cluster.

### 3.1.2 Cluster Catch Digraphs using Ripley’s $K$ Function

While the silhouette index improves the robustness of KS-CCDs, some limitations remain, such as the inability to capture spatial distributions and the need for an unknown input density parameter  $\delta$  [37]. To address this, Manukyan and Ceyhan [37] replaced the KS-type statistic with the Ripley’s  $K$  function [48], denoted as  $K(t)$ , to determine whether the points within each covering ball follow a *homogeneous Poisson process* (HPP). This test is referred to as the *Spatial Randomness Monte Carlo Test* (SR-MCT) with Ripley’s  $K$  function.

The RK-CCD method sets the radius of each covering ball to the largest value for which the points inside the ball pass the SR-MCT, ensuring that the points encapsulated conform to a CSR pattern. The primary difference between RK-CCDs and KS-CCDs is in the determination of the radii, which is now based on Ripley’s  $K$  function rather than the KS-type statistic. Subsequent steps, such as reducing cover complexity using an approximate MDS and refining clusters with the silhouette index, remain the same as in KS-CCDs.

A variant of RK-CCDs introduced by Manukyan and Ceyhan [37] allows for the detection of clusters with arbitrary shapes by considering the connected components of the intersection graph  $G_{MD}$  as the final clusters instead of using the MDS.



## 4 Cluster Catch Digraphs using the Nearest Neighbor Distance

### 4.1 The Limitations of RK-CCDs for Clustering

The Monte Carlo analysis in [53] reveals that outlier detection methods using U-MCCDs and SU-MCCDs exhibit low True Negative Rates (TNRs) for regular points in high-dimensional data sets. This degradation is attributed to the limitations of RK-CCDs in high-dimensional spaces, where dominating covering balls are not sufficiently large for latent clusters.

Specifically, RK-CCDs present two key limitations [53]: (1) The initial points in the SR-MCT are not random, as they are always the centers of the covering balls, leading to inaccurate testing results, especially in high-dimensional data sets; (2) In SR-MCT, the point-wise confidence band for  $K(t)$  is constructed on fixed  $t$  values [37], which is not appropriate for high-dimensional data sets, where the distances between any two points increase substantially.

### 4.2 The SR-MCT with the Nearest Neighbor Distance

To avoid the limitations of RK-CCDs, we have introduced a new CCD approach in [53], which conduct SR-MCT with the *Nearest Neighbor Distance* (NND) instead of the Ripley's  $K$  function.

Given a data set  $\mathcal{X} = \{x_1, x_2, \dots, x_n\}$ , the mean NND of  $\mathcal{X}$  is  $\bar{d} = \frac{\sum_{i=0}^n d_i}{n}$ , where  $d_i$  represents the distance of  $x_i$  to its nearest neighbor. We aim to compare  $\bar{d}$  with the expected mean NND (denoted as  $\mu_d$ ) under the assumption of CSR. A normality test offers a convenient way to obtain P-values for  $\bar{d}$ . Because both  $\mu_d$  and  $\sigma_{\bar{d}}$  (the standard deviation of  $\bar{d}$  under the assumption of CSR) can be derived [10, 11]. However, when the sample size  $n$  is small, the distribution of  $\bar{d}$  is skewed, making the normality test unfeasible [5]. Fortunately, a Monte Carlo test proposed by Besag and Diggle [5] provides an alternative, where the P-values are determined by the empirical quantiles.

Consequently, we have proposed another CCD approach based on the SR-MCT with NND. Additionally, we made several meaningful key enhancements to improve the robustness and reliability of the new CCDs [53]: (1) **Multiple Comparison with Holm's Correction**: Both the median and mean NND are considered for multiple comparisons, with a Holm's Step-Down Procedure for correction [61]; (2) **Descending Radius Test-**

**ing:** Larger covering balls are preferred for high-dimensional data sets. Therefore, we offer the option to test the candidate values for the radius in descending order; (3) **Lower-Tailed Test:** The test is lower-tailed as the upper tail is less relevant when the point pattern is significantly “regular”. (4) **Exclusion of Center Points:** The center points are excluded from the test as they are not random.

The new clustering approach based on CCDs and NND is called *Uniformity- and Neighbor-based CCD* (UN-CCD) clustering method, which is presented in Algorithm 3. It is worth noting that the only difference among KS-CCDs, RK-CCDs, and UN-CCDs is how to determine the radius of covering balls. The time and space complexities of UN-CCDs are  $O((N + d + \log n)n^2 + n^3)$  and  $O(n^2)$  respectively [53].

---

**Algorithm 3: (UN-CCD Clustering Algorithm)** Cluster Catch Digraphs based on the Nearest Neighbor Distance (NND).  $\alpha$  is the level of the Monte Carlo test with NND.

---

**Input:**  $\alpha$ , data set  $\mathcal{X} = \{x_1, x_2, \dots, x_n\}$ ;  
**Output:** Cluster centers of  $\mathcal{X}$ ;  
**Algorithm Steps:**

- 1 **foreach**  $x_i \in \mathcal{X}$  **do**
- 2     Calculate distances  $D(x_i) = \{d(x_i, x_j) | x_j \in \mathcal{X}, x_i \neq x_j\}$ ;
- 3     **foreach** distance  $r_{(j)}$  in  $D(x_i)$  sorted **do**
- 4         Perform the SR-MCT with NND on  $B(x_i, r_{(j)})$ ;
- 5         **if** test rejected at level  $\alpha$  **then**
- 6             Set  $r_{x_i} = r_{(j-1)}$ ; **break**;
- end**
- end**
- end**
- 7 Construct a CCD  $D = (V, A)$  using the pre-determined radii;
- 8 Find the approximate minimum dominating set  $\hat{S}(V)$  in  $D$  with the Greedy Algorithm 1;
- 9 Create intersection graph  $G_{MD} = (V_{MD}, E_{MD})$  with  $\hat{S}(V)$ ;
- 10 Find an approximate minimum dominating set  $\hat{S}(G_{MD})$  in  $G_{MD}$  using the Greedy Algorithm 2 with a score function measuring the number of points covered, stops when the average silhouette index  $sil(P)$  is maximized;
- 11 Output  $\hat{S}(G_{MD})$  as cluster centers;

---

The clustering procedure with UN-CCDs for a 2-dimensional data set consisting of 5 clusters is illustrated in Figure 1.

In Section 5, we compare the performance of KS-CCDs, RK-CCDs, and UN-CCDs with synthetic data sets consists of multiple clusters. We show the advantage of UN-CCDs over RK-CCDs on Gaussian clusters and high-dimensional space.

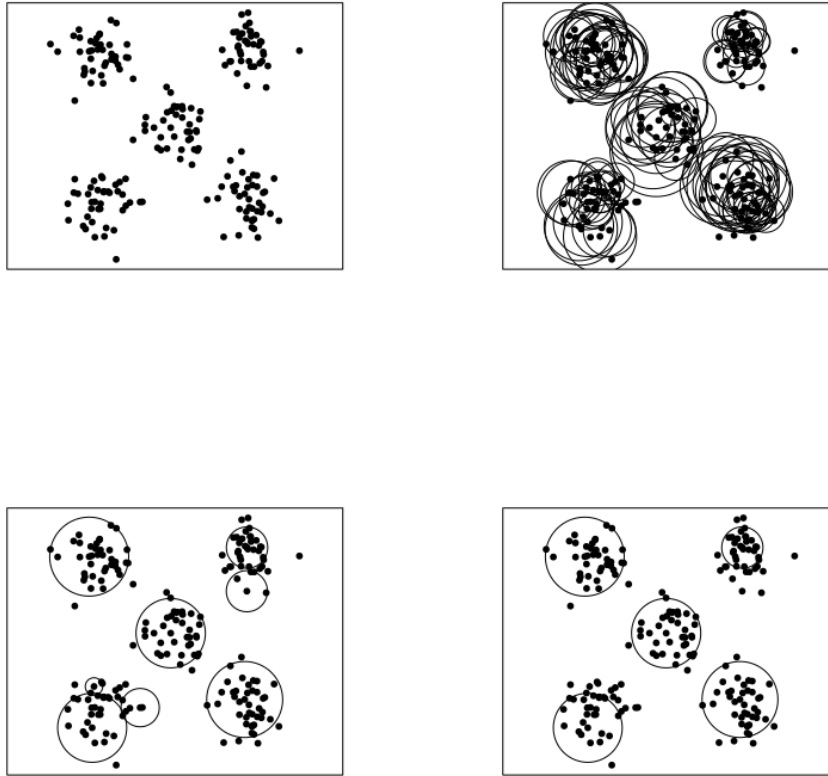


Figure 1: A illustration of clustering with UN-CCDs. Top-left: A data set consisting of 5 clusters generated from 5 different bivariate normal distributions. Top-right: The covering balls of an approximate MDS obtained by Greedy Algorithm 1. Bottom-left: The covering balls of an approximate MDS of the intersection graph. Bottom-right: The dominating covering balls of the intersection graph that maximize silhouette index  $sil(P)$ .

## 5 Monte Carlo Experiments for CCD-based Clustering

This section presents a Monte Carlo Analysis of CCD-based clustering using synthetic data sets. These data sets are generated with varying dimensionality  $d$ , data set size  $n$ , number of clusters, and cluster volumes.

Similar to the design of simulations in [53], the analysis begins with data sets consisting of uniform clusters.

The varied simulation factors are enumerated as follows:

- i. Dimensionality ( $d$ ): 2, 3, 5, 10, 20;
- ii. Data set size ( $n$ ): 50, 100, 200, 500;

iii. Number of clusters (# clusters): 2, 3, 5.

Additionally, all simulated data sets share the following common factors:

- i. Cluster radii is a random variable between 0.8 and 1.2 (uniformly distributed);
- ii. Equal cluster sizes (with varying support volumes and intensities due to the changing radii);

Additionally, the cluster centers are: (1) 1<sup>st</sup> cluster:  $\boldsymbol{\mu}_1 = (\underbrace{3, \dots, 3}_d)$ ; (2) 2<sup>nd</sup> cluster:  $\boldsymbol{\mu}_2 = (6, \underbrace{3, \dots, 3}_{d-1})$ ; (3) 3<sup>rd</sup> cluster:  $\boldsymbol{\mu}_3 = (6, 6, \underbrace{3, \dots, 3}_{d-2})$ ; (4) 4<sup>th</sup> cluster:  $\boldsymbol{\mu}_4 = (3, 5.5, \underbrace{3, \dots, 3}_{d-2})$ ; (5) 5<sup>th</sup> cluster:  $\boldsymbol{\mu}_5 = (8.5, \underbrace{3, \dots, 3}_{d-1})$ . The minimal distances between the first three cluster centers are 3, ensuring well separate clusters. On the other hand, the distances between the 1<sup>st</sup> and the 4<sup>th</sup>, the 2<sup>nd</sup> and the 5<sup>th</sup> cluster centers are 2.5, leading in closer clusters, which may be confused as one cluster by many clustering methods. This study investigates the robustness of the three CCD-based clustering methods to clusters close in proximity. We present three realizations with different number of clusters under 2-dimensional space in Figure 2.



Figure 2: Realizations of the simulation settings with 2, 3, and 5 uniform clusters in  $\mathbb{R}^2$ .

Clustering quality is assessed using both internal and external validation measures, including the Adjusted Rand Index (ARI) [30], the average silhouette index (Sil) [49], and the frequency of successfully identifying the corrected number of clusters (denoted as success rate or % for simplicity). To mitigate the impact of randomness, we repeat each simulation 500 times, and the average measures across these repetitions are recorded.

RK-CCDs are “nearly” parameter-free, requiring only the significance level  $\alpha$  of SR-MCT (with Ripley’s  $K$  function). To accommodate for different dimensions, we set  $\alpha$  to 1% for  $d < 10$  and 0.1% for  $d \geq 10$ , improving the performance of RK-CCDs. For UN-CCDs,

the  $\alpha$  of the SR-MCT (with NND) is set to  $\{15\%, 10\%, 5\%, 1\%, 0.1\%\}$  as  $d$  increases from 2 to 20. Unlike RK-CCDs and UN-CCDs, KS-CCDs require a density parameter  $\delta$  for the KS-based statistic. To manage the scale of  $\delta$  in high-dimensional settings, We work on the value of  $\sqrt[d]{\delta}$  instead, and select the  $\sqrt[d]{\delta}$  maximizing the average silhouette index in each simulation, presented in Table 2 and 6. The simulation results are summarized in Table 1, 3, and 4.

KS-CCDs		$d = 2$			$d = 3$			$d = 5$			$d = 10$			$d = 20$		
		ARI	Sil	%	ARI	Sil	%	ARI	Sil	%	ARI	Sil	%	ARI	Sil	%
$n = 50$	2 clusters	0.997	0.698	0.998	0.999	0.665	1.000	0.999	0.632	1.000	1.000	0.608	1.000	1.000	0.594	1.000
	3 clusters	0.984	0.680	0.964	0.996	0.654	0.998	0.999	0.627	1.000	1.000	0.600	1.000	1.000	0.584	1.000
	5 clusters	0.879	0.603	0.622	0.922	0.584	0.772	0.972	0.565	0.922	0.998	0.546	0.998	1.000	0.536	1.000
$n = 100$	2 clusters	1.000	0.698	1.000	1.000	0.665	1.000	1.000	0.634	1.000	1.000	0.606	1.000	1.000	0.591	1.000
	3 clusters	0.999	0.687	0.998	0.999	0.654	1.000	1.000	0.625	1.000	1.000	0.598	1.000	1.000	0.585	1.000
	5 clusters	0.952	0.619	0.860	0.962	0.590	0.900	0.989	0.567	0.976	0.999	0.547	1.000	1.000	0.535	1.000
$n = 200$	2 clusters	1.000	0.698	1.000	1.000	0.666	1.000	1.000	0.631	1.000	1.000	0.606	1.000	1.000	0.589	1.000
	3 clusters	1.000	0.688	1.000	1.000	0.655	1.000	1.000	0.626	1.000	1.000	0.600	1.000	1.000	0.587	1.000
	5 clusters	0.983	0.625	0.966	0.990	0.596	0.980	0.996	0.570	1.000	1.000	0.548	1.000	1.000	0.535	1.000
$n = 500$	2 clusters	1.000	0.696	1.000	1.000	0.666	1.000	1.000	0.634	1.000	1.000	0.604	1.000	1.000	0.590	1.000
	3 clusters	1.000	0.687	1.000	1.000	0.656	1.000	1.000	0.627	1.000	1.000	0.599	1.000	1.000	0.587	1.000
	5 clusters	0.997	0.633	0.996	0.999	0.598	1.000	0.999	0.570	1.000	1.000	0.547	1.000	1.000	0.535	1.000

Table 1: The simulation results of KS-CCDs on a set of synthetic data sets consisting of uniform clusters.

Density Parameter: $\sqrt[d]{\delta}$		$d = 2$	$d = 3$	$d = 5$	$d = 10$	$d = 20$
$n = 50$	2 clusters	3.70	2.00	1.30	0.75	0.49
	3 clusters	3.10	1.80	1.20	0.700	0.55
	5 clusters	2.60	1.60	1.10	0.800	0.69
$n = 100$	2 clusters	5.20	2.50	1.50	0.80	0.53
	3 clusters	4.40	2.40	1.30	0.78	0.56
	5 clusters	3.80	2.10	1.30	0.88	0.70
$n = 200$	2 clusters	7.00	3.00	1.50	0.85	0.60
	3 clusters	5.90	3.10	1.50	0.82	0.57
	5 clusters	5.40	2.70	1.50	0.98	0.74
$n = 500$	2 clusters	11.00	3.90	1.70	0.88	0.62
	3 clusters	9.00	3.50	1.90	0.85	0.60
	5 clusters	8.40	3.70	1.90	1.10	0.72

Table 2: The optimal scaled densities ( $\sqrt[d]{\delta}$ ) of KS-CCDs on synthetic data sets consisting of uniform clusters.

By optimizing  $\delta$  for each simulation setting, KS-CCDs consistently deliver superior performance, yielding ARI values and success rates (%) close to 1 across most simulation settings, resulting in high average silhouette indices (consistently above 0.55). However, in certain cases when  $n = 50$ , KS-CCDs exhibit reduced efficacy when dealing with 5 clusters. For example, when  $d = 2$  and  $n = 50$ , the success rate (%) declines from 0.998 to 0.622 as the number of clusters increases from 2 to 5. This decrease can be attributed to a drop in the intensities of individual clusters. Furthermore, the small proximity of the 4<sup>th</sup> and 5<sup>th</sup> clusters to the existing clusters increases the likelihood of these clusters being

RK-CCDs		$d = 2$			$d = 3$			$d = 5$			$d = 10$			$d = 20$		
		ARI	Sil	%	ARI	Sil	%	ARI	Sil	%	ARI	Sil	%	ARI	Sil	%
$n = 50$	2 clusters	0.982	0.692	0.998	0.999	0.665	1.000	0.997	0.630	0.992	0.988	0.596	0.960	0.833	0.444	0.474
	3 clusters	0.906	0.655	0.844	0.990	0.651	0.988	0.998	0.625	0.994	0.972	0.589	0.920	0.681	0.424	0.382
	5 clusters	0.517	0.484	0.082	0.810	0.556	0.424	0.967	0.563	0.908	0.994	0.544	0.968	0.801	0.473	0.410
$n = 100$	2 clusters	0.999	0.697	1.000	0.999	0.665	1.000	0.999	0.633	0.998	0.979	0.584	0.922	0.834	0.437	0.454
	3 clusters	0.992	0.684	0.988	0.999	0.654	0.998	0.996	0.624	0.990	0.951	0.576	0.852	0.684	0.433	0.302
	5 clusters	0.768	0.567	0.302	0.938	0.585	0.792	0.982	0.564	0.958	0.956	0.531	0.796	0.511	0.373	0.080
$n = 200$	2 clusters	0.999	0.698	1.000	1.000	0.666	1.000	1.000	0.631	1.000	0.972	0.576	0.892	0.758	0.384	0.288
	3 clusters	1.000	0.688	1.000	0.999	0.655	1.000	1.000	0.626	1.000	0.912	0.560	0.740	0.597	0.376	0.312
	5 clusters	0.926	0.610	0.748	0.988	0.595	0.968	0.993	0.568	0.976	0.917	0.513	0.626	0.595	0.391	0.130
$n = 500$	2 clusters	1.000	0.696	1.000	1.000	0.669	1.000	1.000	0.634	1.000	0.976	0.579	0.910	0.787	0.419	0.428
	3 clusters	0.999	0.686	1.000	1.000	0.654	1.000	1.000	0.627	1.000	0.929	0.571	0.806	0.592	0.394	0.208
	5 clusters	0.997	0.632	1.000	0.999	0.600	1.000	0.999	0.570	1.000	0.865	0.498	0.494	0.439	0.344	0.082

Table 3: The simulation results of RK-CCDs on a set of synthetic data sets consisting of uniform clusters.

UN-CCDs		$d = 2$			$d = 3$			$d = 5$			$d = 10$			$d = 20$		
		ARI	Sil	%	ARI	Sil	%	ARI	Sil	%	ARI	Sil	%	ARI	Sil	%
$n = 50$	2 clusters	0.980	0.691	0.996	0.996	0.664	1.000	0.999	0.632	1.000	1.000	0.608	1.000	0.992	0.585	0.968
	3 clusters	0.926	0.658	0.902	0.981	0.649	0.972	0.999	0.626	1.000	1.000	0.600	1.000	0.991	0.580	0.972
	5 clusters	0.610	0.511	0.214	0.795	0.549	0.480	0.951	0.560	0.872	0.996	0.546	0.992	0.991	0.531	0.944
$n = 100$	2 clusters	0.992	0.695	0.998	0.999	0.665	1.000	1.000	0.634	1.000	1.000	0.606	1.000	0.957	0.545	0.840
	3 clusters	0.988	0.682	0.988	0.998	0.654	1.000	0.999	0.625	0.998	0.999	0.598	0.998	0.899	0.540	0.726
	5 clusters	0.847	0.583	0.604	0.935	0.582	0.836	0.986	0.565	0.976	0.998	0.546	0.992	0.957	0.521	0.802
$n = 200$	2 clusters	0.989	0.694	0.996	0.999	0.665	1.000	1.000	0.631	1.000	1.000	0.606	1.000	0.962	0.547	0.848
	3 clusters	0.994	0.685	0.998	0.999	0.655	1.000	1.000	0.626	1.000	0.998	0.600	0.996	0.921	0.558	0.802
	5 clusters	0.937	0.608	0.858	0.982	0.592	0.968	0.996	0.560	0.996	0.998	0.547	0.990	0.750	0.460	0.284
$n = 500$	2 clusters	0.992	0.693	0.998	1.000	0.666	1.000	1.000	0.634	1.000	1.000	0.604	1.000	0.962	0.548	0.850
	3 clusters	0.991	0.682	1.000	1.000	0.655	1.000	1.000	0.627	1.000	0.997	0.597	0.990	0.851	0.525	0.610
	5 clusters	0.978	0.624	0.974	0.996	0.597	0.998	0.999	0.570	1.000	0.997	0.545	0.982	0.844	0.477	0.438

Table 4: The simulation results of UN-CCDs on a set of synthetic data sets consisting of uniform clusters.

erroneously confused as one. Fortunately, when  $n \geq 100$ , KS-CCDs exhibit substantial improvement in handling 5-cluster data sets.

Although RK-CCDs are not as effective as KS-CCDs across lower-dimensional settings ( $d \leq 5$ ), they still maintain ARI values and success rates above 0.9 in most scenarios, indicating solid performance in low-dimensional space. However, similar to the behavior of KS-CCDs, RK-CCDs also suffer performance degradation in certain cases when there are 5 clusters. For instance, when  $d = 2$  and  $n = 50$ , the success rate (%) drops drastically from 0.998 to 0.082 as the number of clusters increases from 2 to 5, attributable to the low intensities of individual clusters. Additionally, The effectiveness of RK-CCDs declines across high-dimensional space. When  $d = 10$ , the success rates (%) decrease substantially, reaching a minimum of 0.494 for 5-cluster data sets when  $n = 500$ . This deterioration is further exacerbated when  $d = 20$ , with ARIs falling below 0.8 and success rates (%) smaller than 0.4 in most settings.

Under low-dimensional space ( $d \leq 5$ ), UN-CCDs demonstrate comparable performance to RK-CCDs, achieving ARIs and success rates exceeding 0.95 in most settings. Furthermore, UN-CCDs exhibit substantial improvement over RK-CCDs in high-dimensional

space. When  $d = 10$ , both ARIs and success rates approach 1, much higher than those achieved by RK-CCDs. The performance gap between RK-CCDs and UN-CCDs becomes even more pronounced when  $d = 20$ . For example, with 3-cluster data sets where  $n = 200$ , UN-CCDs yield performance metrics of 0.921 (ARI), 0.558 (Sil), and 0.802 (success rate), respectively. These values are substantially higher than the corresponding 0.597, 0.376, and 0.312 obtained by RK-CCDs. This improvement is attributed to the newly developed SR-MCT with NND.

Assuming CSR, UN-CCDs and RK-CCDs perform well with uniform clusters. To evaluate the performance of CCD-based clustering methods on non-uniform data, we conduct simulations with Gaussian clusters. Each Gaussian cluster has a covariance matrix  $\Delta * I_d$ , where  $\Delta$  is a random uniform variable between 0.8 and 1.2, and  $I_d$  represents a  $d \times d$  identity matrix. All other settings, including dimensionality, data size, cluster centers, and the number of clusters, remain the same. Three realizations with different number of Gaussian clusters ( $d = 2$ ) are presented in Figure 3. The simulation results are summarized in Table 5, 7, and 8.

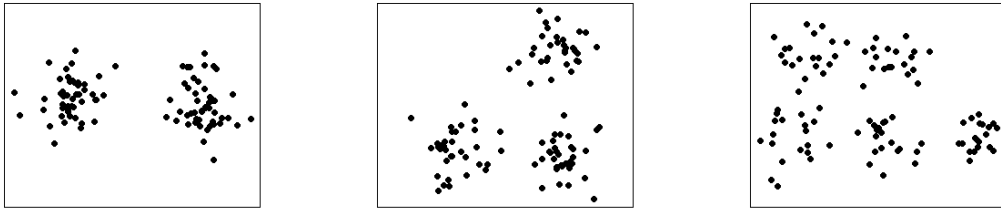


Figure 3: Realizations of the simulation settings with 2, 3, and 5 Gaussian clusters in  $\mathbb{R}^2$ .

KS-CCDs		$d = 2$			$d = 3$			$d = 5$			$d = 10$			$d = 20$		
		ARI	Sil	%	ARI	Sil	%	ARI	Sil	%	ARI	Sil	%	ARI	Sil	%
$n = 50$	2 clusters	0.983	0.704	1.000	0.980	0.633	1.000	0.974	0.537	1.000	0.947	0.399	1.000	0.798	0.247	0.960
	3 clusters	0.973	0.688	0.984	0.970	0.619	0.986	0.960	0.524	0.970	0.880	0.381	0.832	0.685	0.251	0.470
	5 clusters	0.936	0.644	0.890	0.921	0.569	0.872	0.865	0.470	0.718	0.651	0.338	0.376	0.380	0.244	0.050
$n = 100$	2 clusters	0.980	0.704	1.000	0.987	0.635	1.000	0.982	0.540	1.000	0.960	0.399	0.998	0.846	0.256	0.980
	3 clusters	0.985	0.693	1.000	0.981	0.621	0.996	0.978	0.527	0.996	0.926	0.383	0.920	0.713	0.254	0.508
	5 clusters	0.963	0.652	0.986	0.962	0.582	0.982	0.939	0.475	0.936	0.717	0.341	0.556	0.303	0.249	0.000
$n = 200$	2 clusters	0.988	0.703	1.000	0.988	0.634	1.000	0.987	0.539	1.000	0.970	0.402	1.000	0.878	0.261	0.982
	3 clusters	0.988	0.694	1.000	0.988	0.623	1.000	0.984	0.527	1.000	0.963	0.389	0.988	0.736	0.257	0.550
	5 clusters	0.977	0.657	0.998	0.973	0.581	0.998	0.965	0.481	0.988	0.778	0.342	0.704	0.263	0.254	0.000
$n = 500$	2 clusters	0.990	0.703	1.000	0.991	0.637	1.000	0.989	0.541	1.000	0.978	0.404	1.000	0.905	0.266	0.998
	3 clusters	0.989	0.691	1.000	0.990	0.625	1.000	0.988	0.528	1.000	0.976	0.391	0.996	0.793	0.258	0.652
	5 clusters	0.981	0.658	1.000	0.980	0.586	1.000	0.974	0.483	1.000	0.824	0.347	0.776	0.297	0.255	0.000

Table 5: The simulation results of KS-CCDs on a set of synthetic data sets consisting of Gaussian clusters.

Density Parameter: $\sqrt[d]{\delta}$		$d = 2$	$d = 3$	$d = 5$	$d = 10$	$d = 20$
$n = 50$	2 clusters	1.90	1.10	0.60	0.32	0.20
	3 clusters	1.60	0.93	0.52	0.30	0.19
	5 clusters	1.30	0.79	0.46	0.28	0.18
$n = 100$	2 clusters	3.00	1.40	0.71	0.35	0.21
	3 clusters	2.30	1.20	0.65	0.32	0.20
	5 clusters	1.90	0.99	0.58	0.32	0.17
$n = 200$	2 clusters	4.20	1.70	0.76	0.39	0.23
	3 clusters	3.50	1.50	0.71	0.37	0.21
	5 clusters	2.70	1.30	0.66	0.35	0.17
$n = 500$	2 clusters	7.1	2.5	0.95	0.43	0.24
	3 clusters	5.6	2.1	0.90	0.41	0.24
	5 clusters	4.3	1.8	0.82	0.41	0.19

Table 6: The optimal scaled densities ( $\sqrt[d]{\delta}$ ) of KS-CCDs on synthetic data sets consisting of Gaussian clusters.

KS-CCDs		$d = 2$			$d = 3$			$d = 5$			$d = 10$			$d = 20$		
		ARI	Sil	%	ARI	Sil	%	ARI	Sil	%	ARI	Sil	%	ARI	Sil	%
$n = 50$	2 clusters	0.950	0.691	1.000	0.964	0.627	1.000	0.949	0.528	0.994	0.908	0.384	0.978	0.660	0.181	0.628
	3 clusters	0.885	0.659	0.812	0.921	0.607	0.882	0.939	0.517	0.944	0.847	0.372	0.784	0.609	0.212	0.304
	5 clusters	0.627	0.535	0.232	0.760	0.521	0.448	0.812	0.453	0.646	0.654	0.328	0.452	0.396	0.222	0.078
$n = 100$	2 clusters	0.982	0.702	1.000	0.980	0.632	1.000	0.972	0.536	0.998	0.917	0.381	0.958	0.664	0.181	0.630
	3 clusters	0.963	0.685	0.962	0.971	0.617	0.984	0.961	0.521	0.978	0.875	0.370	0.814	0.498	0.186	0.218
	5 clusters	0.830	0.600	0.594	0.906	0.561	0.798	0.874	0.459	0.802	0.664	0.327	0.462	0.348	0.199	0.046
$n = 200$	2 clusters	0.987	0.702	1.000	0.984	0.633	1.000	0.975	0.535	1.000	0.939	0.387	0.954	0.653	0.170	0.548
	3 clusters	0.983	0.692	0.998	0.982	0.621	0.998	0.972	0.522	0.988	0.887	0.375	0.826	0.553	0.188	0.272
	5 clusters	0.950	0.646	0.934	0.950	0.572	0.932	0.910	0.467	0.870	0.683	0.328	0.500	0.342	0.201	0.048
$n = 500$	2 clusters	0.989	0.702	1.000	0.990	0.633	1.000	0.984	0.540	1.000	0.939	0.383	0.912	0.578	0.152	0.500
	3 clusters	0.988	0.690	1.000	0.987	0.624	1.000	0.982	0.525	0.996	0.878	0.370	0.780	0.432	0.165	0.174
	5 clusters	0.977	0.655	0.994	0.976	0.581	1.000	0.951	0.475	0.960	0.668	0.328	0.454	0.335	0.184	0.066

Table 7: The simulation results of RK-CCDs on a set of synthetic data sets consisting of Gaussian clusters.

While the optimal density parameter  $\delta$  is selected for each simulation setting, KS-CCDs demonstrate reduced effectiveness with Gaussian clusters. In low-dimensional settings ( $d \leq 5$ ), KS-CCDs deliver slightly lower performance compared to the scenarios with uniform clusters. Notably, ARI values and success rates remain high ( $> 0.95$ ), indicating high efficacy even with Gaussian clusters. However, KS-CCDs degrade substantially in high-dimensional settings ( $d \geq 10$ ), particularly with three or more clusters. For example, when  $d = 20$  and  $n = 200$ , KS-CCDs deliver average performance metrics of 0.736 (ARI), 0.257 (Sil), and 0.550 (success rate) for 3-cluster data sets, drastically lower than the corresponding 1, 0.587, and 1 obtained with uniform clusters. This performance decline can be explained by the decreased intensities of Gaussian clusters in high-dimensional space, an effect amplified with a larger number of clusters (e.g., 5 clusters). Moreover, Gaussian clusters are unbounded, further contributes to the performance reduction.

Similar to the simulations with uniform clusters, RK-CCDs generally perform well in low-dimensional space, with ARIs and success rates exceeding 0.9 except certain cases with 5 clusters, where the proximities between clusters and the intensities of individual clusters



UN-CCDs		$d = 2$			$d = 3$			$d = 5$			$d = 10$			$d = 20$		
		ARI	Sil	%	ARI	Sil	%	ARI	Sil	%	ARI	Sil	%	ARI	Sil	%
$n = 50$	2 clusters	0.930	0.683	0.988	0.958	0.625	1.000	0.953	0.530	0.998	0.943	0.395	1.000	0.850	0.249	0.988
	3 clusters	0.868	0.649	0.854	0.910	0.600	0.912	0.939	0.517	0.944	0.864	0.374	0.820	0.740	0.248	0.574
	5 clusters	0.644	0.524	0.346	0.740	0.515	0.470	0.774	0.446	0.578	0.600	0.330	0.320	0.444	0.232	0.136
$n = 100$	2 clusters	0.960	0.695	0.994	0.971	0.630	0.998	0.974	0.537	1.000	0.951	0.394	1.000	0.859	0.248	0.962
	3 clusters	0.941	0.676	0.958	0.959	0.612	0.978	0.963	0.522	0.984	0.917	0.379	0.904	0.765	0.247	0.618
	5 clusters	0.828	0.593	0.670	0.888	0.555	0.816	0.875	0.462	0.810	0.713	0.336	0.554	0.438	0.232	0.128
$n = 200$	2 clusters	0.967	0.696	1.000	0.977	0.631	1.000	0.979	0.537	1.000	0.963	0.399	1.000	0.875	0.254	0.978
	3 clusters	0.967	0.685	0.996	0.972	0.618	0.996	0.978	0.524	1.000	0.955	0.386	0.972	0.758	0.250	0.586
	5 clusters	0.913	0.628	0.902	0.942	0.569	0.950	0.939	0.473	0.952	0.750	0.337	0.648	0.439	0.235	0.134
$n = 500$	2 clusters	0.971	0.697	1.000	0.982	0.635	1.000	0.983	0.540	1.000	0.973	0.402	1.000	0.885	0.253	0.946
	3 clusters	0.968	0.683	0.996	0.981	0.621	1.000	0.981	0.525	1.000	0.965	0.387	0.988	0.799	0.249	0.662
	5 clusters	0.950	0.643	0.984	0.963	0.578	0.994	0.963	0.477	0.998	0.808	0.342	0.760	0.450	0.232	0.140

Table 8: The simulation results of UN-CCDs on a set of synthetic data sets consisting of Gaussian clusters.

are small. For instance, with  $d = 2$ ,  $n = 50$ , and 5 clusters, the performance metrics of RK-CCDs are 0.627 (ARI), 0.535 (Sil), and 0.234 (success rate), respectively. RK-CCDs demonstrate similar behavior in high-dimensional space ( $d \geq 10$ ). Their performance is slightly worse than KS-CCDs when  $d = 10$ , and deteriorate further when  $d = 20$ , increasing the data size does not help. For example, when  $d = 20$  and  $n = 500$ , the ARI and success rate are 0.297 and 0, respectively, due to the limitations of the SR-MCT based on the Ripley’s  $K$  function.

Similar to the previous analysis, UN-CCDs perform similarly to RK-CCDs and KS-CCDs in low-dimensional space ( $d \leq 5$ ), Both ARIs and success rates exceed 0.9 in most scenarios, with a few exceptions observed when dealing with 5 clusters. These results are slightly lower than those obtained with uniform clusters. However, UN-CCDs yield superior overall performance in high-dimensional space ( $d \geq 10$ ). When  $d = 10$ , UN-CCDs deliver comparable performance to KS-CCDs, outperforming RK-CCDs, as evidenced by higher ARIs and success rates. To illustrate, with  $n = 200$ ,  $d = 10$ , and 3 clusters, the ARIs for KS-CCDs, RK-CCDs, and UN-CCDs are 0.963, 0.877, and 0.955, respectively. Furthermore, UN-CCDs exhibit a substantial advantage over the other two CCDs when  $d = 20$ . For example, with  $n = 200$ ,  $d = 20$ , and 5 clusters, the ARIs for KS-CCDs, RK-CCDs, and UN-CCDs are 0.263, 0.342, and 0.439, respectively.

To summarize, KS-CCDs demonstrate the best overall performance with uniform clusters when the optimal density parameter  $\delta$  is selected, achieving ARI and success rates close to 1 in most scenarios, invariant to the dimensionality  $d$ . UN-CCDs exhibit slightly lower performance compared to KS-CCDs, and show a substantial advantage over RK-CCDs when  $d \geq 10$ . All three CCDs perform slightly worse with Gaussian clusters in low-dimensional space ( $d \leq 5$ ), further deteriorate when  $d \geq 10$ , where UN-CCDs outper-

form both RK-CCDs and KS-CCDs. The performance of all three CCDs declines with 5 clusters, particularly when the data size  $n$  is small. This is attributed to the low intensities of individual clusters and the small proximities between clusters.

## 6 Real and Complex Data sets

We assess the performance of three CCD-based clustering methods using real and complex artificial data sets in this section, and compare them with some well-known, established methods. Moreover, we want to explore if UN-CCDs outperform RK-CCDs after multiple enhancements. The data sets, obtained from *UCI Machine Learning Repository* and *Clustering basic benchmark* [16, 22], are generally more complex and challenging than the data sets used in Sections 5. To prevent features with larger values from dominating, we preprocess the data sets by normalizing them (except the synthetic data sets including asymmetric, R15, and D31).

The details of each data set are summarized below. Moreover, we present the asymmetric, R15, and D31 data sets in Figure 4.

### Brief descriptions of each data set.

- *iris*: A data set of iris plant, containing 3 types of 50 instances for each.
- *seeds*: The measurements of geometrical properties of kernels belonging to 3 different wheat varieties.
- *knowledge*: Measures the students' knowledge of Electrical DC Machines, categorized into 4 levels.
- *wholesale*: This data set refers to clients of a wholesale distributor, it includes the clients' annual spending on diverse product categories, and are grouped to 3 regions.
- *asymmetric*: A synthetic 2-dimensional data sets with 5 elliptical Gaussian clusters of unbalanced cluster size and intensities, and the inter-cluster distances varies [47].
- *R15* and *D31*: Synthetic data sets consist of 15 or 31 similar Gaussian clusters [55]

We compare the performance of CCDs with established clustering algorithms, *Density Based Spatial Clustering of Applications with Noise* (DBSCAN) [19], the *Minimal Spanning Tree* (MST) Method [63], *Spectral Clustering* (Spectral) [40], *K-means++* [3], and *Louvain Clustering Method* (Louvain) [8].

	$n$	$d$	# of clusters
iris	150	4	3
seeds	210	7	3
knowledge	258	6	4
wholesale	440	8	3
R15	600	2	15
asymmetric	1000	2	5
D31	3100	2	31

Table 9: The size ( $n$ ), dimensionality ( $d$ ), and contamination level of each real-life data set.

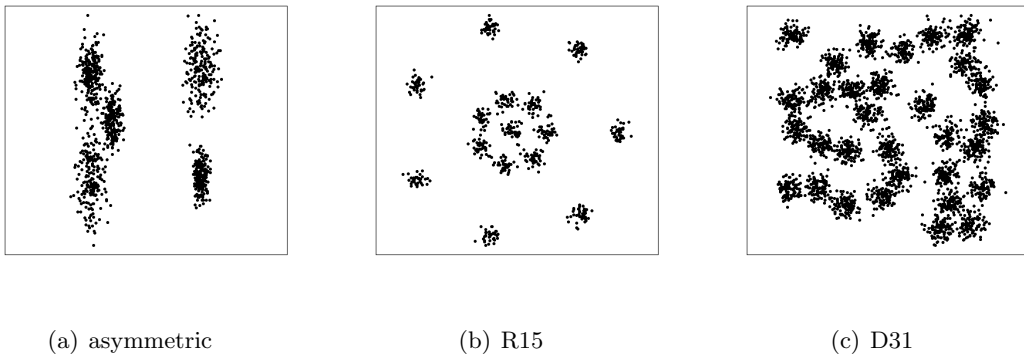


Figure 4: The figures of asymmetric, R15, and D31 data sets

DBSCAN is a density-based clustering method proposed by Ester *et al.* [19], often used to handle data sets with noise or outliers. It identifies clusters by finding “seeds”, which are the points deep inside clusters that have a minimum number (denoted as  $MinPts$ ) of neighbors within a given radius (denoted as  $Eps$ ). After that, it constructs clusters by finding all the points that are *density-reachable* from seeds. Finally, the points not connected to any seeds are labeled as noise or outliers.  $MinPts$  and  $Eps$  are the two input parameters, we follow a heuristic offered by Ester *et al.*, which sets  $MinPts$  to 4, and find the value at the first “elbow” of the sorted 4-dist (the distance of a point to its 4<sup>th</sup> nearest neighbor) plot, setting it to  $Eps$  [19].

The MST clustering method employs a graph-based approach [63]. This method involves constructing a graph by connecting all data points with the minimum sum of edge weights, typically represented by the distance between two points. Subsequently, edges with significantly larger weights than their adjacent edges’ average weight are identified as “inconsistent” and removed. This removal effectively breaks the MST into subtrees, each representing a distinct cluster. We set the threshold value for “inconsistent” edges to 2, which delivers better overall performance compared to other thresholds.

Spectral clustering is a powerful method, employing eigenvalue decomposition of the Laplacian matrix, which are derived from the similarity matrix of the data set [40]. Finally, it applies a traditional method for clustering, and we choose  $K$ -means in this experiment, with the number of clusters known.

$K$ -means++ enhances the classic  $k$ -means clustering method [3]. Sensitivity to the initial chosen cluster centroids is a key weakness of  $k$ -means,  $k$ -means++ address this limitation by selecting initial centroids that are far apart leading to better and stable clustering results and faster convergence. Similar to spectral clustering, we conduct  $k$ -means++ with the number of clusters known.

Louvain clustering method is a greedy algorithm finding communities in large networks [8]. It merges communities or nodes recursively by maximizing the “modularity”, which is a measure of the quality of a partition. The algorithm stops until no further improvement in modularity can be found. Although having an optional resolution parameter affects the size and number of communities, the basic Louvain clustering method does not require any input parameters. In this experiment, we employ the standardized Gaussian kernel to construct a network for the data set and apply Louvain clustering method with the default resolution parameter (i.e., 1).

Consider the CCD-based methods, we tune the significance level  $\alpha$  of SR-MCT for RK-CCDs and UN-CCDs. Specifically,  $\alpha$  is set to 1% for both methods. For KS-CCDs, we choose the  $\sqrt[4]{\delta}$  value that maximizes the average silhouette index in each data set.

We choose Adjust Rand index and Silhouette Index as external and internal validation measures. Furthermore, we record the number of clusters detected by each method. The performance of all methods are summarized in Table 10.

	iris ( $k=3$ )			seeds ( $k=3$ )			knowledge ( $k=3$ )			wholesale ( $k=3$ )			asymmetric ( $k=5$ )			R15 ( $k=15$ )			D31 ( $k=31$ )		
	ARI	Sil	$k$	ARI	Sil	$k$	ARI	Sil	$k$	ARI	Sil	$k$	ARI	Sil	$k$	ARI	Sil	$k$	ARI	Sil	$k$
KS-CCDs	0.561	0.578	2	0.497	0.468	2	0.005	0.254	2	-0.013	0.765	2	0.691	0.643	4	0.989	0.753	15	0.948	0.574	31
RK-CCDs	0.557	0.393	3	0.500	0.164	3	0.052	0.119	2	-0.002	0.344	2	0.730	0.605	4	0.993	0.753	15	0.814	0.495	30
UN-CCDs	0.599	0.445	3	0.509	0.467	2	0.091	0.158	2	0.002	0.113	3	0.736	0.606	4	0.975	0.742	15	0.799	0.474	31
DBSCAN	0.544	0.517	2	0.003	0.121	1	0.005	0.198	1	0.006	0.569	1	0.467	0.548	3	0.936	0.702	15	0.350	0.343	15
MST	0.530	-0.145	6	0.000	-0.364	4	0.003	-0.089	3	0.004	-0.491	13	0.785	-0.160	12	0.536	-0.071	65	0.511	-0.199	276
K-mean++	0.590	0.459	3*	0.773	0.404	3*	0.202	0.169	4*	-0.007	0.446	3*	0.882	0.645	5*	0.894	0.678	15*	0.912	0.547	31*
Spectral	0.555	0.475	3*	0.679	0.349	3*	0.189	0.120	4*	-0.012	0.446	3*	0.975	0.623	5*	0.899	0.611	15*	0.778	0.332	31*
Louvain	0.630	0.436	3	0.722	0.394	3	0.149	0.155	5	-0.004	0.243	6	0.805	0.479	8	0.604	0.644	10	0.371	0.446	9

Table 10: The performance of selected clustering algorithms on real and complex data sets. ARI: Adjust Rand Index; Sil: Silhouette Index;  $k$ : number of clusters ( $k$  is the input parameter for K-mean++ and spectral clustering);  $\hat{k}$ : estimated number of clusters.

All the methods obtain comparable ARIs on the iris data set. Precisely, Louvain and UN-CCDs attain the highest ARIs of 0.630 and 0.599, respectively. KS-CCDs and DBSCAN produce the best Sils. RK-CCDs, UN-CCDs, and Louvain clustering method

correctly identify the true number of clusters.

In the seeds data set, K-means++, spectral clustering, and Louvain clustering method perform better than other methods when considering ARI. Meanwhile, UN-CCDs and KS-CCDs achieve the highest Sils of 0.468 and 0.467, respectively, indicating better-defined cluster structures. Both RK-CCDs and Louvain clustering method successfully identify the correct number of clusters.

In the knowledge data set, The performance of all the methods is generally mediocre. K-mean++ and spectral clustering get the highest ARIs, 0.202 and 0.189, respectively. KS-CCDs and DBSCAN produce the best Sils. MST is the only method that identified 3 clusters.

All the methods perform poorly on the wholesale data set, Suggested by the ARIs, which are around 0, indicating the clustering results akin to random assignment. Therefore, we turn to Sil for evaluation, KS-CCDs and DBSCAN outperform other methods, achieving Sil of 0.765 and 0.569, respectively. Despite having the second-lowest Sil score, UN-CCDs is the only method that correctly identifies the number of clusters.

When the number of clusters is known, K-means++ and spectral clustering exhibit the best performance. These methods achieve ARI values of 0.882 and 0.975, respectively, and Sil values of 0.645 and 0.623, respectively. The CCD-based methods show slightly lower performance, with ARI and Sil around 0.7 and 0.6, respectively. However, these methods identify 4 clusters, the closest to the actual number.

The three CCD-based algorithms perform better than the other methods on the R15 data set, they successfully capture 15 Gaussian clusters, achieving ARIs close to 1 and Sils around 0.75. DBSCAN, K-means++, and spectral clustering deliver slightly inferior performance, with ARIs around 0.9 and Sils around 0.65.

Consider the D31 data set, KS-CCDs and K-means++ detect all 31 clusters, deliver the highest ARIs of over 0.9, outperforming other methods. RK-CCDs and UN-CCDs also perform well, with ARI scores of 0.814 and 0.799, respectively. They detect 30 and 31 clusters, respectively, outperforming all other methods except KS-CCDs and K-means++.

In summary, KS-CCDs demonstrate the best overall performance, obtaining the highest Sil and competitive ARI across almost all data sets. However, identifying the best density parameter  $\delta$  for the KS-based statistic is computationally expensive. Even when the number of clusters is provided as an input parameter for K-means++ and spectral clustering, RK-CCDs and UN-CCDs maintain comparable performance, making them

competitive clustering methods. DBSCAN and Louvain clustering method yield slightly worse results than the five methods mentioned above. MST consistently produces negative ARI or Silhouette scores, indicating the worst performance among the evaluated methods.

## 7 Summary and Conclusion

In this paper, we propose a new CCD-based method for clustering, called UN-CCDs, which uses the NND instead of the Ripley’s  $K$  function to conduct the spatial randomness test.

UN-CCDs address the limitation of RK-CCDs in high-dimensional clustering, attributes to several enhancements discussed in Section 4.2. Through extensive Monte Carlo simulation in Section 5, we demonstrate that UN-CCDs are, in general, comparable to RK-CCDs in low-dimensional space, and deliver superior performance when the dimensionality  $d \geq 10$ . This is evidenced by the substantially higher Adjust Rand Index and the success rate in identifying the correct number of clusters. Moreover, as shown by the real and complex data analysis in Section 6, UN-CCDs maintain comparable performance to RK-CCDs and state-of-the-art methods such as spectral clustering and K-means++ (which require the number of clusters as an input parameter). These findings establish UN-CCDs as a robust and versatile clustering method, suitable for a wide range of data dimensionality and complexity.

## 8 Acknowledgements

Most of the Monte Carlo simulations in this paper were completed in part with the computing resource provided by the Auburn University Easley Cluster. The authors are grateful to Artür Manukyan for sharing the codes of KS-CCDs and RK-CCDs.

## References

- [1] Rakesh Agrawal, Johannes Gehrke, Dimitrios Gunopulos, and Prabhakar Raghavan. Automatic subspace clustering of high dimensional data for data mining applications. In *Proceedings of the 1998 ACM SIGMOD International Conference on Management of Data*, pages 94–105, 1998.
- [2] Mihael Ankerst, Markus M Breunig, Hans-Peter Kriegel, and Jörg Sander. Optics: Ordering points to identify the clustering structure. *ACM Sigmod Record*, 28(2):49–60, 1999.
- [3] David Arthur and Sergei Vassilvitskii. k-means++: The advantages of careful seeding. Technical report, Stanford, 2006.
- [4] Adelchi Azzalini and Giovanna Menardi. Clustering via nonparametric density estimation: The r package pdfcluster. *ArXiv Preprint ArXiv:1301.6559*, 2013.
- [5] Julian Besag and Peter J Diggle. Simple monte carlo tests for spatial pattern. *Journal of the Royal Statistical Society Series C: Applied Statistics*, 26(3):327–333, 1977.
- [6] Kevin Beyer, Jonathan Goldstein, Raghu Ramakrishnan, and Uri Shaft. When is “nearest neighbor” meaningful? In *Database Theory—ICDT’99: 7th International Conference Jerusalem, Israel, January 10–12, 1999 Proceedings 7*, pages 217–235. Springer, 1999.
- [7] David M Blei, Andrew Y Ng, and Michael I Jordan. Latent dirichlet allocation. *Journal of Machine Learning Research*, 3(Jan):993–1022, 2003.
- [8] Vincent D Blondel, Jean-Loup Guillaume, Renaud Lambiotte, and Etienne Lefebvre. Fast unfolding of communities in large networks. *Journal of Statistical Mechanics: Theory and Experiment*, 2008(10):P10008, 2008.
- [9] Vasek Chvatal. A greedy heuristic for the set-covering problem. *Mathematics of Operations Research*, 4(3):233–235, 1979.
- [10] Philip J Clark and Francis C Evans. Distance to nearest neighbor as a measure of spatial relationships in populations. *Ecology*, 35(4):445–453, 1954.
- [11] Philip J Clark and Francis C Evans. Generalization of a nearest neighbor measure of dispersion for use in  $k$  dimensions. *Ecology*, 60(2):316–317, 1979.

- [12] Dorin Comaniciu and Peter Meer. Mean shift: A robust approach toward feature space analysis. *IEEE Transactions on Pattern Analysis and Machine Intelligence*, 24(5):603–619, 2002.
- [13] Arthur P Dempster, Nan M Laird, and Donald B Rubin. Maximum likelihood from incomplete data via the em algorithm. *Journal of the Royal Statistical Society: Series B (methodological)*, 39(1):1–22, 1977.
- [14] Jason G DeVinney. *The class cover problem and its applications in pattern recognition*. PhD thesis, Johns Hopkins University, 2003.
- [15] Harold Edson Driver and Alfred Louis Kroeber. *Quantitative expression of cultural relationships*, volume 31. Berkeley: University of California Press, 1932.
- [16] Dheeru Dua and Casey Graff. Uci machine learning repository, 2017.
- [17] Joseph C Dunn. A fuzzy relative of the isodata process and its use in detecting compact well-separated clusters. 1973.
- [18] Michael B Eisen, Paul T Spellman, Patrick O Brown, and David Botstein. Cluster analysis and display of genome-wide expression patterns. *Proceedings of the National Academy of Sciences*, 95(25):14863–14868, 1998.
- [19] Martin Ester, Hans-Peter Kriegel, Jörg Sander, and Xiaowei Xu. A density-based algorithm for discovering clusters in large spatial databases with noise. In *Proceedings of the Second International Conference on Knowledge Discovery and Data Mining (KDD-96)*, volume 96, pages 226–231, Portland, Oregon, USA, 1996. AAAI Press.
- [20] Absalom E Ezugwu, Abiodun M Ikotun, Olaide O Oyelade, Laith Abualigah, Jeffrey O Agushaka, Christopher I Eke, and Andronicus A Akinyelu. A comprehensive survey of clustering algorithms: State-of-the-art machine learning applications, taxonomy, challenges, and future research prospects. *Engineering Applications of Artificial Intelligence*, 110:104743, 2022.
- [21] Douglas H Fisher. Knowledge acquisition via incremental conceptual clustering. *Machine Learning*, 2:139–172, 1987.
- [22] Pasi Fränti and Sami Sieranoja. K-means properties on six clustering benchmark datasets, 2018.



- [23] Guojun Gan, Chaoqun Ma, and Jianhong Wu. *Data clustering: theory, algorithms, and applications*. Society for Industrial and Applied Mathematics, China, 2020.
- [24] James Gareth, Witten Daniela, Hastie Trevor, and Tibshirani Robert. *An introduction to statistical learning: with applications in R*. Springer, New York City, New York, 2013.
- [25] Michelle Girvan and Mark EJ Newman. Community structure in social and biological networks. *Proceedings of the National Academy of Sciences*, 99(12):7821–7826, 2002.
- [26] Sudipto Guha, Rajeev Rastogi, and Kyuseok Shim. Cure: An efficient clustering algorithm for large databases. *ACM Sigmod Record*, 27(2):73–84, 1998.
- [27] Sudipto Guha, Rajeev Rastogi, and Kyuseok Shim. Rock: A robust clustering algorithm for categorical attributes. *Information Systems*, 25(5):345–366, 2000.
- [28] Alexander Hinneburg, Daniel A Keim, et al. *An efficient approach to clustering in large multimedia databases with noise*, volume 98. Bibliothek der Universität, Konstanz, Germany, 1998.
- [29] Dorit S Hochbaum. Approximation algorithms for the set covering and vertex cover problems. *SIAM Journal on Computing*, 11(3):555–556, 1982.
- [30] Lawrence Hubert and Phipps Arabie. Comparing partitions. *Journal of Classification*, 2:193–218, 1985.
- [31] Richard M Karp. Reducibility among combinatorial problems. In *Complexity of Computer Computations*, pages 85–103. Springer, 1972.
- [32] George Karypis, Eui-Hong Han, and Vipin Kumar. Chameleon: Hierarchical clustering using dynamic modeling. *Computer*, 32(8):68–75, 1999.
- [33] Leonard Kaufman and Peter J Rousseeuw. *Finding groups in data: an introduction to cluster analysis*. John Wiley & Sons, 2009.
- [34] Raghuram Krishnapuram and James M Keller. The possibilistic c-means algorithm: insights and recommendations. *IEEE Transactions on Fuzzy Systems*, 4(3):385–393, 1996.
- [35] James MacQueen. Classification and analysis of multivariate observations. In *5th Berkeley Symp. Math. Statist. Probability*, pages 281–297, 1967.

- [36] Artür Manukyan and Elvan Ceyhan. Classification of imbalanced data with a geometric digraph family. *The Journal of Machine Learning Research*, 17(1):6504–6543, 2016.
- [37] Artür Manukyan and Elvan Ceyhan. Parameter free clustering with cluster catch digraphs (technical report). *ArXiv Preprint ArXiv:1912.11926*, 2019.
- [38] David J Marchette. *Random graphs for statistical pattern recognition*. John Wiley & Sons, Hoboken, New Jersey, 2005.
- [39] Glenn W Milligan and Martha C Cooper. An examination of procedures for determining the number of clusters in a data set. *Psychometrika*, 50:159–179, 1985.
- [40] Andrew Ng, Michael Jordan, and Yair Weiss. On spectral clustering: Analysis and an algorithm. *Advances in neural information processing systems*, 14, 2001.
- [41] Raymond T Ng and Jiawei Han. Clarans: A method for clustering objects for spatial data mining. *IEEE Transactions on Knowledge and Data Engineering*, 14(5):1003–1016, 2002.
- [42] Nikhil R Pal, Kuhu Pal, James M Keller, and James C Bezdek. A possibilistic fuzzy c-means clustering algorithm. *IEEE Transactions on Fuzzy Systems*, 13(4):517–530, 2005.
- [43] Carey E Priebe, David J Marchette, Diego Socolinsky, and Jason DeVinney. Classification using class cover catch digraphs. *Journal of Classification*, 20:3–23, 2003.
- [44] Lawrence Rabiner and Biinghwang Juang. An introduction to hidden markov models. *IEEE Assp Magazine*, 3(1):4–16, 1986.
- [45] Xingcheng Ran, Yue Xi, Yonggang Lu, Xiangwen Wang, and Zhenyu Lu. Comprehensive survey on hierarchical clustering algorithms and the recent developments. *Artificial Intelligence Review*, 56(8):8219–8264, 2023.
- [46] Carl Rasmussen. The infinite gaussian mixture model. *Advances in Neural Information Processing Systems*, 12, 1999.
- [47] Mohammad Rezaei and Pasi Fränti. Can the number of clusters be determined by external indices? *IEEE Access*, 8:89239–89257, 2020.

- [48] Brian D Ripley. The second-order analysis of stationary point processes. *Journal of Applied Probability*, 13(2):255–266, 1976.
- [49] Peter J Rousseeuw. Silhouettes: a graphical aid to the interpretation and validation of cluster analysis. *Journal of Computational and Applied Mathematics*, 20:53–65, 1987.
- [50] Amit Saxena, Mukesh Prasad, Akshansh Gupta, Neha Bharill, Om Prakash Patel, Aruna Tiwari, Meng Joo Er, Weiping Ding, and Chin-Teng Lin. A review of clustering techniques and developments. *Neurocomputing*, 267:664–681, 2017.
- [51] Erich Schubert, Jörg Sander, Martin Ester, Hans Peter Kriegel, and Xiaowei Xu. Dbscan revisited, revisited: why and how you should (still) use dbscan. *ACM Transactions on Database Systems (TODS)*, 42(3):1–21, 2017.
- [52] Gholamhosein Sheikholeslami, Surojit Chatterjee, and Aidong Zhang. Wavecluster: a wavelet-based clustering approach for spatial data in very large databases. *The VLDB Journal*, 8(3):289–304, 2000.
- [53] Rui Shi, Nedret Billor, and Elvan Ceyhan. Outlier detection with cluster catch digraphs. *ArXiv Preprint ArXiv:2409.11596*, 2024.
- [54] Thorvald Sorensen. A method of establishing groups of equal amplitude in plant sociology based on similarity of species content and its application to analyses of the vegetation on danish commons. *Biologiske Skrifter*, 5:1–34, 1948.
- [55] Cor J. Veenman, Marcel J. T. Reinders, and Eric Backer. A maximum variance cluster algorithm. *IEEE Transactions on Pattern Analysis and Machine Intelligence*, 24(9):1273–1280, 2002.
- [56] Juha Vesanto and Esa Alhoniemi. Clustering of the self-organizing map. *IEEE Transactions on Neural Networks*, 11(3):586–600, 2000.
- [57] Hongzhi Wang, Mohamed Jaward Bah, and Mohamed Hammad. Progress in outlier detection techniques: A survey. *IEEE Access*, 7:107964–108000, 2019.
- [58] Wei Wang, Jiong Yang, Richard Muntz, et al. Sting: A statistical information grid approach to spatial data mining. In *Vldb*, volume 97, pages 186–195. Citeseer, 1997.

- [59] Joe H Ward Jr. Hierarchical grouping to optimize an objective function. *Journal of the American Statistical Association*, 58(301):236–244, 1963.
- [60] Michel Wedel and Wagner A Kamakura. *Market segmentation: Conceptual and methodological foundations*. Springer Science & Business Media, 2000.
- [61] Daniela Witten and Gareth James. *An introduction to statistical learning with applications in R*. Springer Publication, New York City, New York, 2013.
- [62] Hui Yin, Amir Aryani, Stephen Petrie, Aishwarya Nambissan, Aland Astudillo, and Shengyuan Cao. A rapid review of clustering algorithms. *ArXiv Preprint ArXiv:2401.07389*, 2024.
- [63] Charles T Zahn. Graph-theoretical methods for detecting and describing gestalt clusters. *IEEE Transactions on Computers*, 100(1):68–86, 1971.
- [64] Dao-Qiang Zhang and Song-Can Chen. A novel kernelized fuzzy c-means algorithm with application in medical image segmentation. *Artificial Intelligence in Medicine*, 32(1):37–50, 2004.
- [65] Ji Zhang. Advancements of outlier detection: A survey. *ICST Transactions on Scalable Information Systems*, 13(1):1–26, 2013.
- [66] Ji Zhang, Wynne Hsu, and Mong Li Lee. Clustering in dynamic spatial databases. *Journal of Intelligent Information Systems*, 24(1):5–27, 2005.
- [67] Tian Zhang, Raghu Ramakrishnan, and Miron Livny. Birch: an efficient data clustering method for very large databases. *ACM Sigmod Record*, 25(2):103–114, 1996.